Characterization of Mozambique's Vulnerability to Coastal Erosion

Patrícia Filipa Barradas Domingos, patricia.domingos@tecnico.ulisboa.pt
Master student in Environmental Engineering, Instituto Superior Técnico

Abstract

Coastal erosion is identified as one of the most important processes affecting the Mozambican coast. With 44% of the country's population living in coastal areas, there is a serious need to better understand and quantify the changes imposed by this phenomenon. Moreover, is fundamental to infer about the vulnerability the coast is subject to. The main objective of this thesis is to make use of remote sensing and GIS techniques to study the evolution and vulnerability of the Mozambican coast throughout a period of 26 years (1989-2015), using Landsat satellite imagery. To achieve this objective an attempt was made to estimate coastline changes in terms of erosion and/or accretion in the country, more specifically along the Sofala Bay region, through the implementation of two different classification methods based on support vector machines (SVMs) and modified normalized difference water index (MNDWI), with posterior coastline extraction. Sites where changes deemed more significant were identified, change analysis was performed by the computation of erosion and accretion areas to have a better understanding of actual area lost or gained. Vulnerability was computed by the application of the coastal vulnerability index (CVI) in this sites. It was possible to conclude that extensive erosion and coastline retreat are occurring in this region even though CVI calculation revealed low to moderate vulnerability, with exception of sites located in the city of Beira, that obtained a high vulnerability value. Possible reasons that could explain the results obtained are also analysed in the process of this study.

Keywords: Mozambique, coastal erosion, remote sensing, Landsat, support vector machines, coastal vulnerability index.

1 Introduction

Coastal erosion has been identified as one of the most important phenomena occurring in the Mozambican coastal system, mainly due to natural forces. It is known that 44% of the country's population is living in coastal areas, and with the ever increasing trend for urbanization and tourism infrastructures, which exerts intensified pressure on coastal environments, it becomes so very important to study the processes that occur along the coast (Palalane and Juízo, 2015). Due to the importance of this processes, rapid and reliable techniques are necessary to monitor the coastline and develop viable plans to protect it and reduce potential losses (Ghosh et al., 2015). The main objective of this thesis is to make use of remote sensing and GIS techniques to study the evolution and vulnerability of the Mozambican coast throughout a period of 26 years, using Landsat satellite imagery. A specific study area was chosen, located within the Sofala province and along the Sofala Bay. To achieve the objective proposed, coastline changes were estimated in terms of erosion and/or accretion, through the implementation of two different classification methods, MNDWI and SVMs, and posterior visual analysis. After extraction

and overlaying of every coastline, areas where changes occur were quantified in terms of area lost or gained. For this sites, a coastal vulnerability index (CVI) was developed based on three parameters (coastline change rate, landuse and population density), in order to map the relative vulnerability of these sites, characterizing the coastal processes and activities that may be affecting the coastal areas.

2 Case study

The region chosen to perform deeper analysis is located within the Sofala province and between latitude 19°30 S and 21°10 S, approximately (Figure 1). This area is located in the central region of Mozambique and includes the city of Beira, which is referred in the literature as a very vulnerable city to erosion (MICOA, 2007; Palalane and Juízo, 2015). It also includes part of the Sofala Bay extending from the Save river to the region of Tama. This region is clearly considered a high risk area affected by direct and indirect anthropogenic pressure, such as tourism development and the construction of damns, and naturally induced erosion. NAPA (2007), identified the centre of high vulnerability to erosion in the Mozambican coast to be around 20° latitude, which encompasses the Sofala Bay, and a little south of Beira city. Cyclone hazard in this region is also characterized as very high, with several incidents reported in the literature (INGC, 2009; Palalane and Juízo, 2015). High tides also contribute to increasing effects of erosion in this region, since tidal amplitudes along the coast can reach and even exceed the 6 meters, the highest values obtained along the Mozambican coast (Palalane and Juízo, 2015; Hoguane, 2007).

Figure 1: Area of study delimited within the Sofala Province, Mozambique. Acquired from Google Earth™.

3 Methodology

3.1 Datasets

For the purpose of this study five images of Landsat Thematic Mapper (TM) and one from Landsat 8 were used (Table 1). All images were obtained and downloaded from the United States Geological Survey (USGS) archive, (`http://earthexplorer.usgs.gov/`). The images were acquired at Level-1T processing which means they were already geometrically corrected, resampled and registered to a UTM 36 WGS84 ellipsoid with elevation correlation applied (USGS, 2016). As reported by NASA, this product is georeferenced with a level of precision better than 0.44 pixels (meaning 13.4 m) (Petropoulos et al., 2015). Due to this characteristics, it was deemed, after careful visual analysis using ENVI software environment, that the images were ready to be used as is and no further pre-processing

regarding georeferencing or radiometric calibration would be employed.

Table 1: Landsat data used in this study and respective characteristics.

Satellite/Data	Path/Row	Date	Local Hour	Resolution	Level	Cloud Cover (%)
Landsat 5 TM	167/74	19/09/1989	07:07	30m	L1T	0
Landsat 5 TM	167/74	31/05/1995	06:48	30m	L1T	0.06
Landsat 5 TM	167/74	30/08/1999	07:19	30m	L1T	0
Landsat 5 TM	167/74	24/06/2004	07:23	30m	L1T	0
Landsat 5 TM	167/74	20/08/2007	07:35	30m	L1T	0.03
Landsat 8	167/74	06/05/2015	07:41	30m	L1T	0.02*

*This cloud cover value corresponds to the cloud cover on Land.

When considering the images to use, tidal predictions and tide heights were also taken into account. This data was acquired from SHOM, a French website that provides historic calculations of water level by hour for different Port locations around the world (`http://maree.shom.fr/`). In this case Beira Port was used for the estimations. It was possible to infer that for all images, high tide was occurring and differences in tide heights of about 1 meter between years were not significant enough to induce major changes when performing coastline delineation.

3.2 Processing

To classify the images and delineate the coastline, two different approaches were followed: (1) discrimination of land and water interface through the use of the MNDWI, and (2) a semi-automatic image classification method based on SVMs. The **MNDWI water index** was calculated by combining the green and mid-infrared bands, (MNDWI=(Green-MIR)/(Green+MIR)). After employing this index, histogram thresholding was performed and images with 2 classes, "land" and "water", were obtained. **SVMs** was implemented in two steps. First, pixels were collected separately for each of the images through the selection of regions of interest (ROIs) representing each class, "land" and "water". Secondly, a multi-class pair wise classification was implemented where SVMs was applied. This pair wise classification was performed using a non-linear kernel function, the Radial Basis Function (RBF), from which results images classified in two classes (Petropoulos et al., 2015). From the classified images obtained, for both methods, coastlines were possible to be extracted and visualized using ArcMap software. After validation of the results obtained, areas that reflected higher changes in terms of erosion and/or accretion were identified, and coastline change detection analysis and the CVI were computed.

3.3 CVI

The CVI is calculated based on the risk values assigned to each of the input parameters and computed as the square root of the product of all ranked variables and divided by the total number of variables (n) (Jana and Bhattacharya, 2013). Equation 1 represents the CVI.

$$CVI = \sqrt{\frac{[a \cdot b \cdot c]}{3}} \tag{1}$$

Where a= risk rating assigned to coastline change rate; b= risk rating assigned to land-use cover and c= risk rating assigned to population density.

In this study and following the work done by Jana and Bhattacharya (2013), three risk variable were considered - coastline change rate, landuse and population density. **Coastline change rate** was computed making use of the Digital Shoreline Analysis System (DSAS 4.3) developed by the USGS in 2010. Transects were cast at 100 meter interval and historical rates of coastline change were then calculated for each transect using end point rate (EPR) statistics. This method is calculated by dividing the distance of coastline change by the time elapse between the oldest and the most recent coastline, in this case approximately 26 years (Himmelstoss, 2009). **Landuse** types were grouped and ranked according to economic value. This was done based on a subjective assessment of which landuse types were more or less valuable, specially to humans (McLaughlin et al., 2002). For the purposes of this present study, data from DINAGECA (Direcção Nacional de Geografia e Cadástro) of Mozambique, was used to assess landuse. Regarding **population density**, census data from 2007, obtained from Mozambique Instituto Nacional de Estatística, was used to evaluate and classify this parameter. For each province, census data available was divided by the respective area and population density obtained. Data relative to the area of each province, was obtained from DINAGECA of Mozambique, last updated in 2009. The three parameters were classified and ranked based on Jana and Bhattacharya (2013) and McLaughlin et al. (2002). Table 2 presents the risk ratings assigned to each variable.

Table 2: Vulnerability classification, adapted from Jana and Bhattacharya (2013).

	Risk Rating			
Variables	**Low (1)**	**Moderate (2)**	**High (3)**	**Very High (4)**
Coastline Change Rate (m/year)	>10	0 - 10	-10 - 0	<-10
Landuse	Bare soils River banks	Mangroves Meadows	Salt Pans Agricultural lands	Urbanized, Semi-urbanized dwelling areas Industrialized area
Population density (people/km^2)	< 500	501 - 1000	1001 - 1500	>1500

3.4 Validation of the Results

Results were validated with Google Earth^{TM} images as well as the Eolian Mapping Index (EMI). The first could only be used for the images from the most recent years (2004, 2007 and 2015). The **EMI** is an index that uses the red and near-infrared spectral bands to generate an image that emphasizes areas with low vegetation density and high soil reflectance. The near-infrared (NIR) and red (R) spectral bands combined with the ratio of red to near-infrared (R/NIR) were used, respectively, as RGB components to make a color composite (NIR - R - (R/NIR)). In the results obtained it was expected that the brighter tone of yellow represented sand areas, while bright red regions represented areas with high vegetation density (Khiry, 2007). After validation it was possible to conclude that SVMs derived coastlines were more accurate in coastline delineation, contrary to MNDWI derived ones which included some of the intertidal zone, leading to an overestimation of erosion area. This is why for further analysis of the results and computations performed, SVMs delineated coastlines were utilized.

4 Results and Discussion

4.1 Change Detection

To detect changes, the resulting coastlines, from the classified images, were overlaid in ArcGIS 10.0 and coastline positions could be seen for each date (1989, 1995, 1999, 2004, 2007 and 2015). Different colours were given to the coastline of each year in order to make it easier to observe the differences between them (Figure 2).

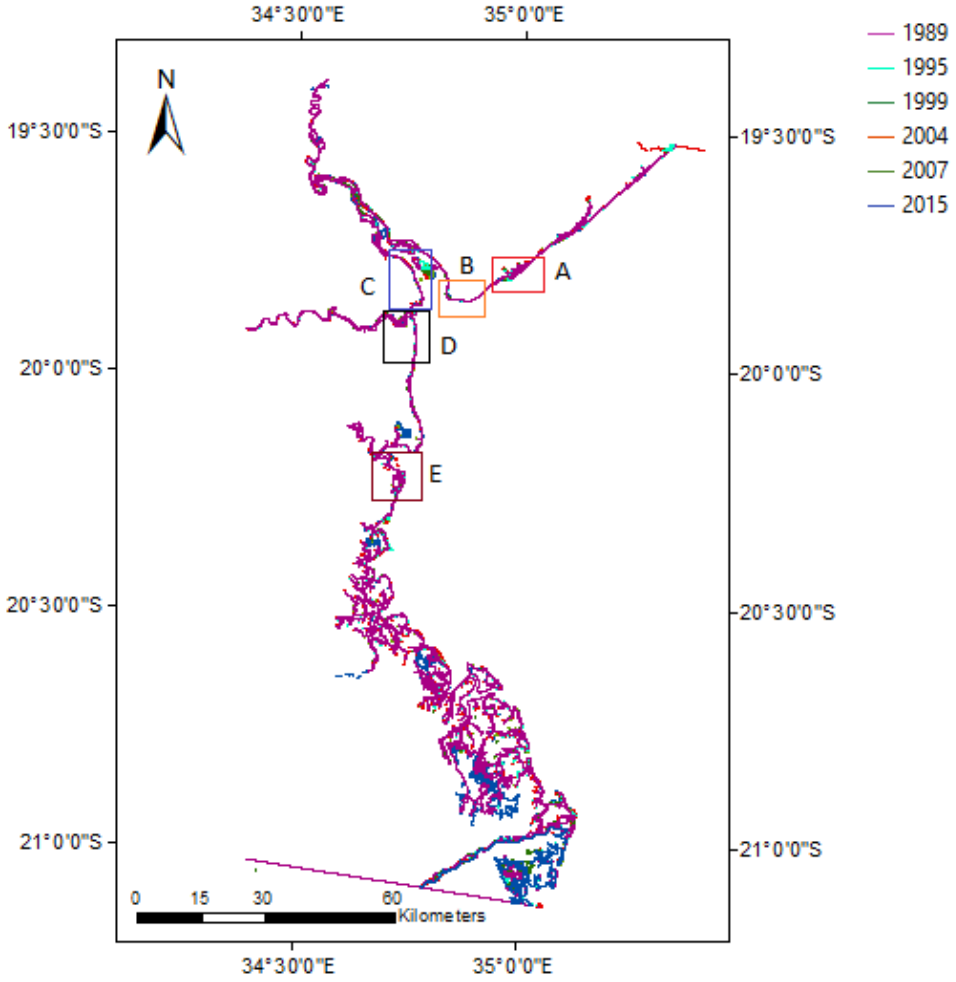

Figure 2: Coastline positions (1989-2015), with sites delimited from A to E.

The obtained coastlines were studied carefully through visual analysis, in order to identify erosion and accretion dominant locations. This was performed while comparing and validating coastline changes with the Landsat source images and EMI index. From this analysis 5 sites (A-E) were identified as the ones where erosion and accretion changes were greater when compared to others. Figure 2 presents the 5 sites chosen. For each site, polygons were created between 1989 and 2015 coastlines in order to create erosion and accretion areas. Red areas represent erosion while green areas represent accretion. Figures 3 and 4 show the results obtained regarding coastline change analysis for site B as an example.

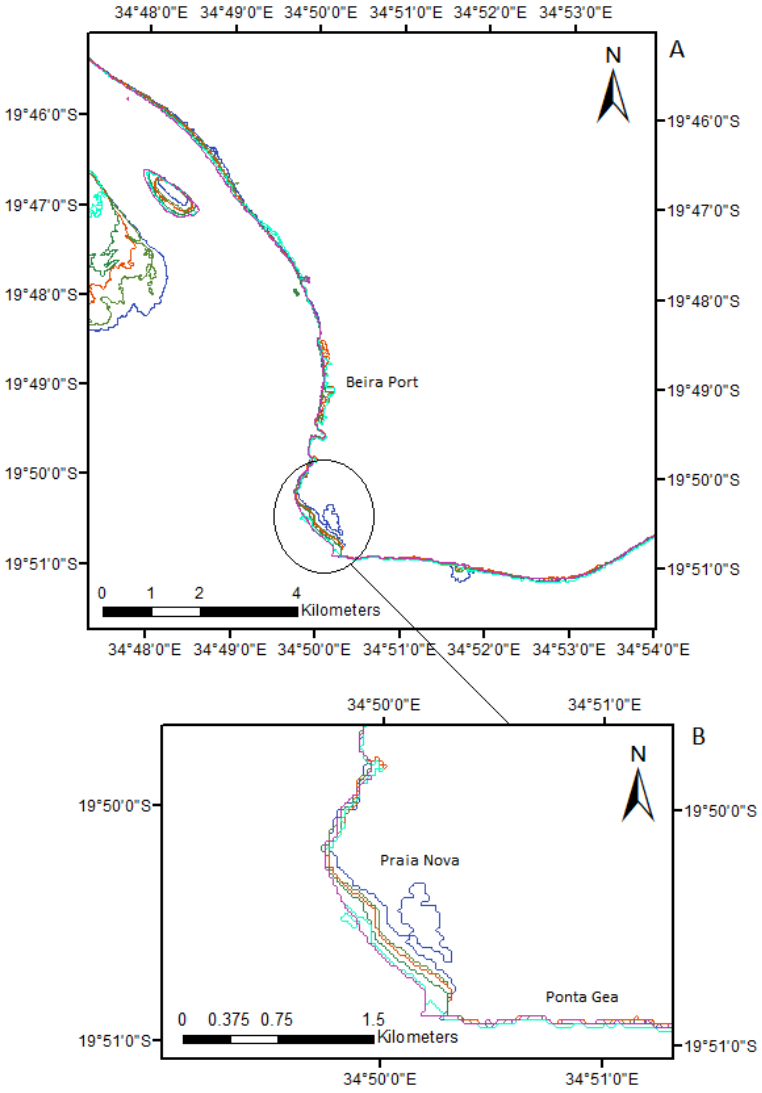

Figure 3: A - Coastline positions (1989-2015), for Zone B; B - Close up of coastline positions for Ponta Gea and Praia Nova regions.

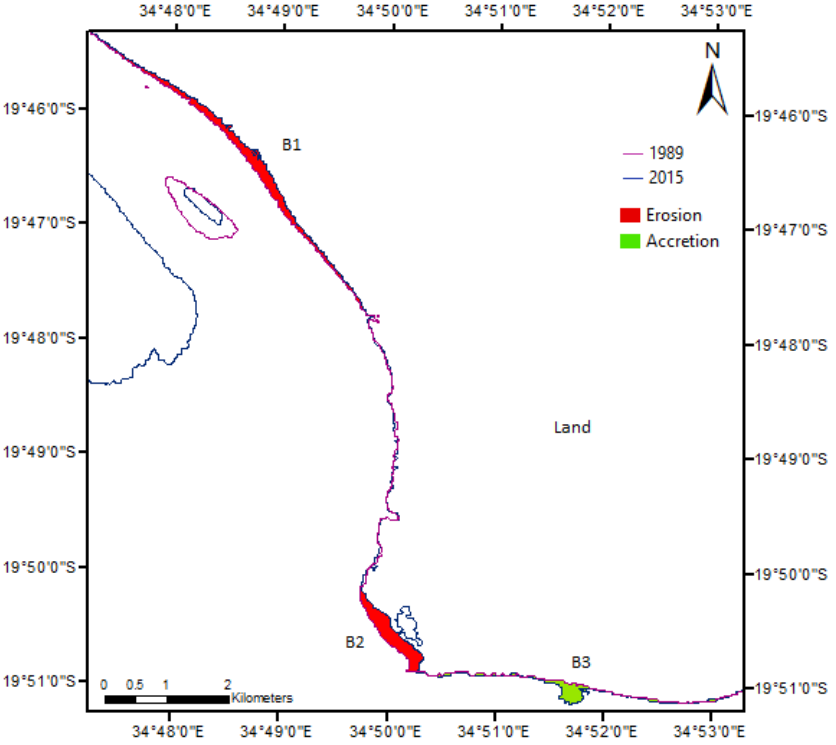

Figure 4: Difference between 1989 and 2015 coastlines, for Zone B.

Analysing figure 3 and 4, one can observe that when erosion is concerned, regression of the coastline occurred through out the years in study, and where accretion occurred, coastline moved seaward through out the years. Erosion in B1 and B2 represented an overall loss in land area, while accretion in B3, was concluded to be due to a movement in sand, clearly visible in the EMI image, where this region was represented with a bright tone of yellow. This increase in sand can be attributed to the construction of groins and seawalls along Ponta Gea over the past years as an attempt to decrease erosion in this region (Palalane et al., 2015). However, some of the field of groins built, also intensified erosion along Praia Nova (B2).

Similar analysis was performed for the rest of the sites represented in figure 2, with results obtained varying in terms of area changed and processes involved. Even though only site B was chosen to be presented here, the trends observed in this site, where also observed in the others. Where recession of the coast related to land movement, including sand regions, occurred, every year the coastline moved further landward. Losses in land area, were due to a loss in sand (A, B and E), bare soil (B), or mangrove disappearance and destruction (B to E). Where accretion occurred, increase in land from one year to the next, was either due to sand movement and accumulation (A and B), or to mangrove establishment and development (C to E). The following table shows the overall change observed, in hectares and hectares per kilometre, for each of the sites studied.

Table 3: Overall change area between 1989 and 2015 for sites A-E.

Site	Approximate coastline stretch size (km)	Erosion (hectares)	Accretion (hectares)	Overall change (hectares)	Overall change (ha/km)
A	29.77	123	60	(-) 63	(-) 2.12
B	21.09	79	17	(-) 62	(-) 2.94
C	25.27	324	76	(-) 248	(-) 9.81
D	9.45	83	0	(-) 83	(-) 8.78
E	53.26	169	111	(-) 58	(-) 1.09

Analysing all 5 sites, it was possible to conclude that overall change was higher in site C, where more hectares were lost for each km of coastline. Site D closely followed with an overall changed area of (-) 8.78ha/km. The remaining sites registered overall changes much lower than site C and D. These high values for the two sites probably mean that the process to which they are subject to, are much stronger and erosion inducing than for the remaining sites. Accretion area revealed to be higher in site E, due to mangrove establishment. Phenomena involved in these changes, of course, depends on the characteristics of each site.

4.2 CVI

After assigning risk classes to each of the parameters, vulnerability maps were obtained for each of the sites studied here (A-E). In order to do this, a 1km buffer, using the 1989 coastline as baseline, was created. The resulting buffer was then intersected with a 500x500 meter Fishnet, which resulted in the area between the buffer and the baseline, being subdivided into polygons. This polygons were classified with a value between 1 and 4, according with the vulnerability classification presented

in table 2. After assigning risk values, CVI was calculated and vulnerability maps computed for each site. Each risk map shows the 1km buffer classified for each parameter and the 1989 coastline. Figure 5 shows this classification and final vulnerability map obtained for site B, as an example.

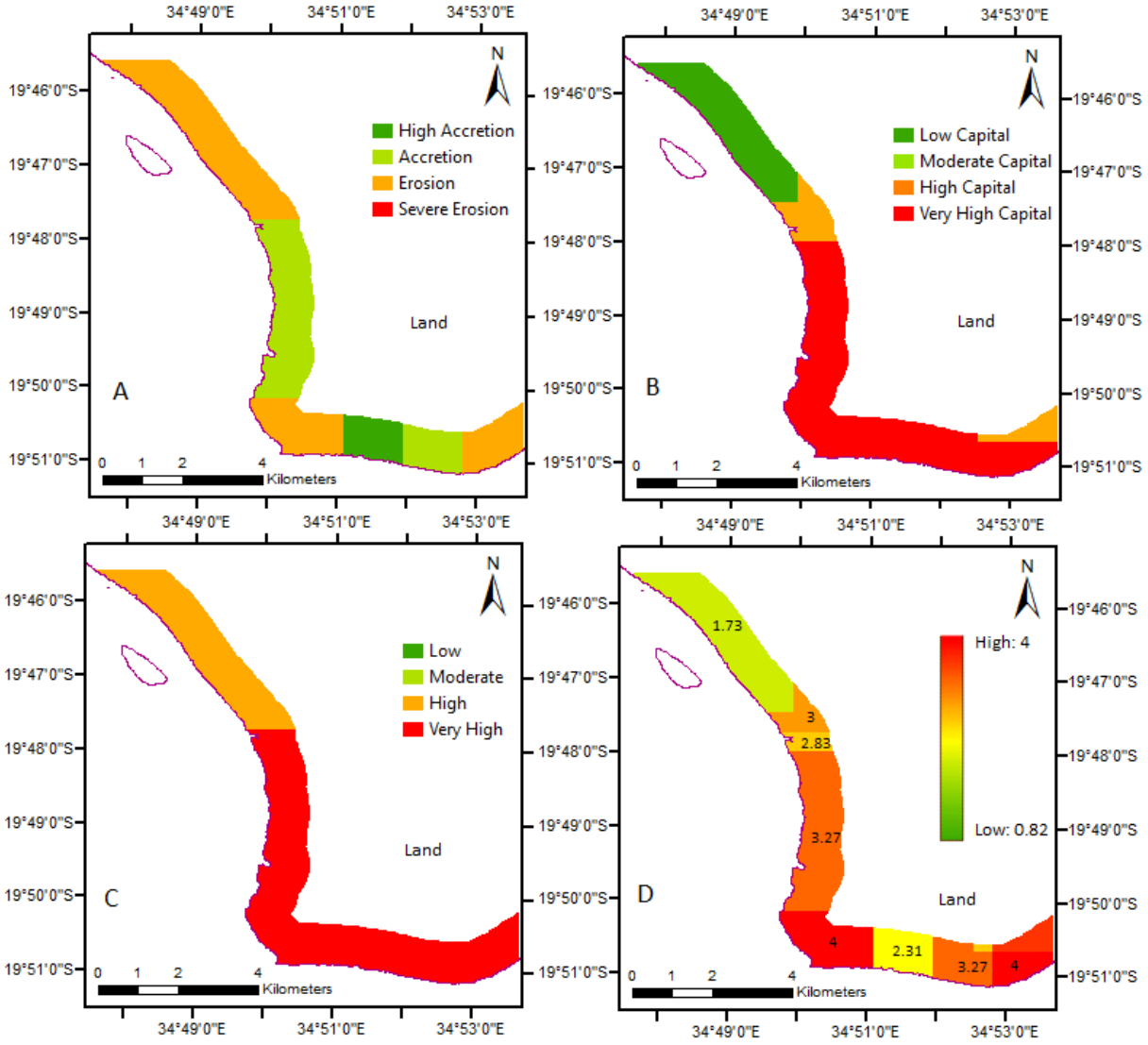

Figure 5: Risk classes for site B; A- Change Rate; B - Landuse; C- Population density. D - Vulnerability Map.

This site was chosen to be presented here since it demonstrates the city of Beira, highly populated and where the greatest vulnerability values were found. Very high capital and very high population density contribute to the values obtained in this site, with maximum vulnerability of 4, being experienced in some of the regions within this site, namely in Praia Nova. From the vulnerability map (Figure 5-D), it was possible to infer that 25.6% of coastline had a vulnerability index of 4, the maximum value, 32.7% a vulnerability of 3.26, 3.4% a vulnerability of 3, 4.1% a vulnerability of 2.83, 8.3% a vulnerability of 2.31 and finally, 25.9% a vulnerability of 1.73. Similar analysis was performed for sites A, and C to E.

In general, except for site A and B that recorded the highest vulnerability values, in all other sites there was an overall vulnerability bellow 2. Even when a few sites experienced severe erosion or high erosion rates, this vulnerability remained bellow 2. In terms of overall change rate, higher values

were observed in site C and E. However, after computation of the CVI, higher vulnerability values were found in site B, since this region corresponds mostly to the city of Beira, where pressure from high population density is intensified. Sites A and B were the ones most conditioned by population density, while sites C to E, were mainly dominated by mangrove forests, with moderate capital landuse, and very low in population density. This is why for these regions the CVI obtained was quite low.

All sites studied here were extremely influenced by tide currents processes, which might have also contributed to the increased erosion observed (Moreira, 2005). Tidal amplitudes that can exceed the 6 meters, observed in Beira and in general throughout the entire Sofala Bank, also contributed to increasing effects of erosion observed along the coast (Palalane et al., 2015; Hoguane, 2007). In the entirety of the region of study, a great portion of area lost was due to mangrove disappearance. In fact, along the Sofala Bank the destruction of overall mangrove forest has been observed to be mainly due to overexploitation, for their wood and non-wood material, which can help further explain why a lot of mangrove area seems to be disappearing (Chevallier, 2013; Hoguane, 2007). Deforestation of mangroves along Sofala Bay was pointed by Sitoe et al. (2014) to be happening at a rate of 4.9% per year, which reveals to be quite alarming, leading to a decrease in the natural protection that mangroves provide against wave erosion action and natural occurring disasters such as cyclones. As such, this disappearance is thought to be the main cause of the great area lost in the sites studied. The great cyclone vulnerability observed over the region of study has also contributed to a decrease in mangrove area and intensified erosion hazard (Palalane and Juízo, 2015).

Change detection maps obtained, give a clearer view of the actual erosion and/or accretion occurring along the Mozambican coast and approximate values of changed area in hectares associated with these phenomena. Vulnerability values obtained for this sites, under the data utilized for this study, are considered be a representation of present and future values, if nothing is done to change it. Taking this into consideration, the vulnerability maps can be used for better understanding of the actual vulnerability the coast is subject to. Hopefully, they can be a source for further and more detailed maps developed in the future that will allow better planning and management of the coastal zone.

5 Conclusions

From this study it was possible to conclude that extensive erosion and coastline retreat are occurring in this region even though CVI calculation revealed mostly low to moderate vulnerability. This results depend entirely on the parameters studied, since they greatly influence the value computed. Including coastal forcing characteristics such as tidal dynamics and sea level rise predictions, may help compute, in a more accurate way, vulnerability of the coast.

This study demonstrated the applicability of remote sensing and GIS techniques for monitoring the coastlines. Integration of aerial photography with high resolution imagery could improve accuracy of the results. However, in regards to this study, Landsat derived images revealed to be very useful and adequate for the scale of the changes that were observed here. Continuous monitoring of the coast is needed in order to understand the changes that coastlines are subject to, and to develop viable plans to protect the coast and reduce potential losses.

References

Chevallier, R. (2013). *Balancing Development and Coastal Conservation : Mangroves in Mozambique*.

Ghosh, M. K., Kumar, L., and Roy, C. (2015). Monitoring the coastline change of Hatiya Island in Bangladesh using remote sensing techniques. *ISPRS Journal of Photogrammetry and Remote Sensing*, 101:137–144.

Himmelstoss, E. (2009). DSAS 4.0 Installation Instructions and User Guide" in: et al. 2009, Digital Shoreline Analysis System (DSAS) version 4.0 — An ArcGIS extension for calculating shoreline change. *U.S. Geological Survey Open-File Report 2008-1278*, 3:79.

Hoguane, A. (2007). Perfil Diagnóstico da Zona Costeira de Moçambique. *Revista da Gestão Costeira Integrada*, 7(1):69–82.

INGC (2009). INGC (Instituto Nacional de Gestão de Calamidades) Climate Change Report: Study on the Impact of Climate Change on Disaster Risk in Mozambique. 34p.

Jana, A. and Bhattacharya, A. K. (2013). Assessment of Coastal Erosion Vulnerability around Midnapur-Balasore Coast, Eastern India using Integrated Remote Sensing and GIS Techniques. *Journal of the Indian Society of Remote Sensing*, 41(3):675–686.

Khiry, M. A. (2007). *Spectral mixture analysis for monitoring and mapping desertification processes in semi-arid areas in North Kordofan State, Sudan*. PhD thesis, University of Heidelberg, Germany.

McLaughlin, S., McKenna, J., and Cooper, J. a. G. (2002). Socio-economic data in coastal vulnerability idices: constrains and opportunities. *Journal of Coastal Research*, 497(36):487–497.

MICOA (2007). Relatório nacional sobre ambiente marinho e costeiro. maputo, moçambique: Ministério para coordenação da acção ambiental–direção nacional de gestão ambiental.

NAPA (2007). National adaptation programme of action (napa), ministry for the co-ordination of environmental affairs, maputo, moçambique. Approved by the Council of Ministers at its 32nd Session.

Palalane, J.; Larson M.; Hanson, H. and Juízo, D. (2015). Coastal erosion in mozambique: Governing processes and remedial measures. 32(3):700–718.

Petropoulos, G. P., Kalivas, D. P., Griffiths, H. M., and Dimou, P. P. (2015). Remote sensing and GIS analysis for mapping spatio-temporal changes of erosion and deposition of two Mediterranean river deltas: The case of the Axios and Aliakmonas rivers, Greece. *International Journal of Applied Earth Observation and Geoinformation*, 35:217–228.

Sitoe, A. A., Mandlate, L. J. C., and Guedes, B. S. (2014). Biomass and carbon stocks of sofala bay mangrove forests. *Forests*, 5(8):1967–1981.

USGS (2016). Geometry. *United States Geoogical Survey (USGS)*. `http://landsat.usgs.gov/geometry.php`,accessed on 22/06/2016.